Activation of the *WT1* tumor suppressor gene promoter by Pea3

Maria Teresa Discenza[a,1], Darryl Vaz[b], John A. Hassell[b], Jerry Pelletier[a,c,*]

[a] *Department of Biochemistry, McIntyre Medical Sciences Building, McGill University, Montreal, QC, Canada H3G 1Y6*
[b] *Institute for Molecular Biology and Biotechnology, McMaster University, 1280 Main Street, Hamilton, ON, Canada L8S 4K1*
[c] *McGill Cancer Center, McIntyre Medical Sciences Building, McGill University, Montreal, QC, Canada H3G 1Y6*

Received 17 November 2003; revised 14 January 2004; accepted 21 January 2004

First published online 4 February 2004

Edited by Lukas Huber

Abstract **Gene array profiling of RNA from cells engineered to express a dominant-negative version of the ETS family member transcription factor Pea3 (polyomavirus enhancer activator 3) identified *WT1* as a candidate downstream gene. Given the co-expression of WT1 and Pea3 in developing kidney and breast tissue undergoing mesenchymal to epithelial transitions, we further characterized this potential gene hierarchy. Analysis of the human *WT1* promoter revealed several potential binding sites for Pea3. Pea3 transactivated the *WT1* promoter in transient transfection assays and bound to specific sites within the *WT1* promoter in vitro. Our results position *Pea3* upstream of *WT1* and define a gene hierarchy important for mesenchymal–epithelial transitions.**

Key words: Pea3; WT1; Tumor suppressor; Wilms' tumor; Gene regulation

1. Introduction

Wilms' tumor is a pediatric renal malignancy of the kidney, affecting approximately 1 in 10 000 children before the age of 5 years [1]. *WT1*, the *Wilms' tumor suppressor 1* gene, was identified on the basis of its mutational inactivation in 10–15% of sporadic Wilms' tumors [2] and in the germline of children with a genetic predisposition to Wilms' tumor [3]. The human *WT1* gene, located at chromosome position 11p13, spans approximately 50 kb of genomic DNA and includes 10 exons which generate four alternatively spliced mRNAs [4]. WT1 protein isoforms contain a proline/glutamine-rich amino-terminus and four zinc finger motifs at the carboxy-terminus [4]. The zinc fingers form the DNA binding domain of WT1 and share homology with the *early growth response 1* (*EGR-1*) gene family of transcription factors. Consequently, WT1 can bind to, and regulate, the expression of numerous genes through the GC-rich EGR-1 consensus binding site (5′-GXGXGGGXG-3′) as well as through a TC-rich site $(5'\text{-TCC-}3')_n$ [5,6]. WT1 has been shown to regulate the expression of several target genes, including those encoding growth factors, growth factor receptors, transcription factors, extracellular/secreted proteins, and cell cycle control proteins [4].

WT1 expression is detected in several tissues during mammalian development and in adulthood [4]. It is expressed during all stages of kidney development, becoming restricted to the podocyte layer of the glomerulus in the mature kidney. During gonadal development, *WT1* is expressed in the urogenital ridge and becomes localized to the Sertoli cells of the testis and the granulosa and epithelial cells of the ovary. Apart from its expression in the kidney and gonads, *WT1* is also detected in the uterus, spleen, liver, thymus, certain areas of the brain and spinal cord, in the abdominal wall musculature, and in the mesothelial linings of organs in the thoracic and abdominal cavities. Other groups have shown that *WT1* is expressed in the stem cells of the bone marrow [7], the developing epicardium [8] and retina [9], and the mammary gland [10,11].

Targeted inactivation of *WT1* in mice revealed that WT1 serves an important role as a transcription factor regulating organogenesis during embryonic development. The mice lacked kidneys, gonads, spleens and adrenal glands, and also had mesothelial and retinal defects [8,9,12,13]. *WT1* null mouse embryos fail to develop a urogenital system and die in utero at E13.5–E15.5 [12] due to heart malformations leading to edema. The initial mesenchymal–epithelial interactions that occur during kidney development are arrested in the *WT1* null embryos due to lack of outgrowth of the epithelial ureteric bud into the metanephric mesenchyme (which normally expresses *WT1*) with subsequent apoptotic death of the mesenchymal cells. The inability of the metanephric mesenchyme from *WT1* null embryos to respond to inductive signals [12], as well as the spatial and temporal expression pattern of *WT1* during kidney development [14,15], implicates WT1 in a unique role controlling mesenchymal–epithelial interactions during development. Although much work has been done to ascertain WT1's role in development and tumorigenesis, little is known about the developmental regulation of *WT1* expression. *WT1* promoter-reporter gene assays have shown that Pax2 and Pax8, members of the paired-box family of transcription factors, as well as the ubiquitous transcriptional regulator Sp1, activate the *WT1* promoter [16–20]. Furthermore, WT1 appears to be involved in an autoregulatory loop where it represses its own expression [21].

Pea3 (polyomavirus enhancer activator 3) is a member of the ETS family of transcription factors [22]. Mouse *Pea3* (the human gene is named *ETS translocation variant 4* [*ETV4*] or *E1A-F*) is the founding member of a subfamily of *ETS* genes,

*Corresponding author. Fax: (1)-514-398 7384.
E-mail address: jerry.pelletier@mcgill.ca (J. Pelletier).

[1] Present address: Institut de recherches cliniques de Montreal, Laboratoire de transcription genique, 110, avenue des Pins Ouest, Local 2640, Montreal, QC, Canada H2W 1R7.

0014-5793/04/$30.00 © 2004 Published by Elsevier B.V. on behalf of the Federation of European Biochemical Societies.
doi:10.1016/S0014-5793(04)00104-8

which also includes *Er81* (*ETV1*) and *Erm* (*ETV5*) (reviewed in [23]). ETS proteins are defined by an evolutionarily conserved, approximately 85 amino acid ETS DNA binding domain which recognizes an ~10 bp motif with a core 5′-GGAA/T-3′ sequence [24]. Sequences flanking this central element govern the specificity of binding by particular ETS proteins. The ETS domain of each protein is sufficient for sequence-specific DNA binding and studies with Pea3 have shown that DNA binding by Pea3 is regulated by intramolecular and intermolecular protein–protein interactions [25,26]. The activation domain of Pea3 subfamily members is located near the amino-terminus and comprises an acidic amino acid region (reviewed in [23]). In particular, the Pea3 activation domain spans amino acids 42–85 of the 480 amino acid protein and is flanked by two regions that independently negatively regulate its activity [25].

The expression patterns of the three Pea3 family members suggest different functions for each gene during mouse embryogenesis and indicate that these genes are expressed in association with proliferation and migration events [27]. Interestingly, the three genes are expressed in organs where mesenchymal–epithelial interactions occur, such as the lung, the salivary gland or the kidney. During development of the kidney, *Pea3* is continuously expressed in ureteric bud ends and their adjacent condensed mesenchyme. Just prior to birth, *Pea3* expression becomes restricted to the mesenchymal compartment in the cortical nephrogenic zone. *Pea3* expression is no longer detectable in the adult kidney.

During the course of a set of gene expression experiments undertaken to identify downstream targets of Pea3, the *WT1* gene scored positive as a putative target. In this report we identify and characterize a segment within the *WT1* promoter that contains two Pea3 sites. Overexpression of *Pea3* transactivates the *WT1* promoter in transient transfection assays and the binding of Pea3 to a specific sequence within the *WT1* promoter appears responsible for this transactivation. Our results suggest an important hierarchy between these two transcription factors during mesenchymal–epithelial interactions in organogenesis.

2. Materials and methods

2.1. Cell lines, transfections, and CAT assays

Mammary carcinoma cell line MDA-MB-468 (ATCC) was grown in Dulbecco's modified Eagle's medium (DMEM) supplemented with 10% heat-inactivated fetal bovine serum, 100 U/ml penicillin, 100 μg/ml streptomycin and 0.25 μg/ml fungizone. Cells were incubated at 37°C in a 5% CO_2, humidified environment. CHO and COS7 cells (ATCC) were grown at 37°C with 5% CO_2 in α-MEM and DMEM, respectively, supplemented with 10% heat-inactivated fetal calf serum, 100 U/ml penicillin, and 100 μg/ml streptomycin. For transactivation assays, 5×10^5 cells were transfected with 5 μg of reporter plasmid and 2–4 μg of expression plasmid by the calcium phosphate precipitation method [16,17]. Each DNA precipitate was adjusted to contain an equal amount of DNA by the addition of the empty expression vector pRcRSV. Transfection efficiency was controlled for by co-transfection of 3 μg of β-actin/*β-galactosidase* in CHO cells and 1 μg of CMV/*β-galactosidase* in COS7 cells. Transfections were performed in duplicate and repeated a minimum of three times. Cells were harvested and assayed for β-galactosidase and chloramphenicol acetyltransferase (CAT) activity 36–48 h post transfection [16,17]. The extent of each CAT reaction was monitored by thin-layer chromatography using silica gel 60 F_{254} plates to separate the acetylated [^{14}C]chloramphenicol from non-acetylated [^{14}C]chloramphenicol. The percent conversion for the CAT reactions was quantitated by direct analysis on a Fujix BAS 2000 phosphoimager.

2.2. Recombinant adenoviruses

Plasmids pMA20 and pBHG10 were generously provided by Dr. Frank L. Graham (McMaster University, Hamilton, ON, Canada). Dominant-negative Pea3 (ΔNPea3En) lacks the activation domain of Pea3 and includes the repression domain of *Drosophila* Engrailed fused to the C-terminus [28]. An adenoviral vector containing ΔNPea3En was constructed by homologous recombination between plasmids pMA20 (carrying ΔNPea3En) and pBHG10 [29]. Ad-STOP-ΔNPea3En carries a loxP-flanked STOP sequence upstream of ΔNPea3En that effectively blocks translation of the transgene transcript. Ad-STOP-ΔNPea3En was passaged through CRE-expressing 293 cells resulting in excision of the STOP sequence and packaging of adenovirus capable of expressing ΔNPea3En [29]. Expression and functional activity of the transgene in MDA-MB-468 cells following infection was confirmed by Western blot and luciferase reporter assay, respectively (Vaz and Hassell, in preparation).

2.3. Microarray analysis

MDA-MB-468 cells were grown to 80% confluence and infected with either Ad-STOP-ΔNPea3En (control) or Ad-ΔNPea3En (experimental). At 12 h post infection, total RNA was harvested using TRIzol (Life Technologies) according to the manufacturer's protocol. RNA was quantified by measuring A_{260} and its quality verified using an Agilent 2100 Bioanalyzer. RNA samples were processed for global gene expression analysis on Affymetrix GeneChip Human Genome HG-U133A arrays (Gene Expression Facility, Ottawa Health Research Institute, Ottawa, ON, Canada). The experiment was repeated three times; one of the control RNA samples failed to be efficiently reverse transcribed during the labeling reaction. Data were processed and analyzed using Microarray Suite 5.0 and Data Mining Tool 3.0. Data from each array were normalized to an average target intensity of 150 to control for variances in labeling and hybridization efficiency. Prior to statistical analysis to identify genes downregulated by ΔNPea3En expression, probe sets with absent calls on the control arrays were omitted. Pairwise comparisons were performed between each of two control and three experimental samples (six comparisons in total), generating a signal log ratio and a *P* value of significant change for each probe set. A *t*-test was also performed on normalized signal intensities for each probe set assuming unequal variances and a normal distribution, generating a *P* value measure of confidence. Fold change was calculated from the ratio of the average of two control samples to the average of three experimental samples.

2.4. Lightcycler data analysis

RNA Master SYBR Green I mix (Roche Molecular Biochemicals) was used to set up the lightcycler polymerase chain reaction (PCR). The amplification program consisted of 1 cycle of 95°C for 30 s, followed by 45 cycles of 95°C with 1 s hold, 57°C annealing with 5 s hold, followed by 72°C with 10 s hold. Acquisition temperature was at 72°C. The amplification was followed by melting curve analysis using the program run for one cycle at 95°C with a 5 s hold, 65°C with 15 s hold, and 95°C with 0 s hold at the step acquisition mode. A negative control without cDNA template was run with every assay to assess the overall specificity.

The mean concentration of β_2-microglobulin was used to control for input cDNA using primers hβ2M/F (5′-CACCCCCACTGAAAAAGATG-3′) and hβ2M/R (5′-GATGCTGCTTACATGTCTCG-3′). The mean β_2-microglobulin cDNA concentration was determined three times for each sample. A standard curve for WT1 was established using a series of two-fold serial dilutions from one of the control samples (Fig. 1C; control #3) using primers hWT1ex7/S (5′-TTCATGTGTGCTTACCCAGG-3′) and hWT1ex8/AS (5′-AGTCCTTGAAGTCACACTGG-3′). The relative levels of WT1 in the other control and experimental samples were then determined from this standard curve and were determined three independent times for each sample.

2.5. Plasmid constructs

The plasmids pCAT/−1101 (containing nucleotides −1101 to +199 of the *WT1* promoter) and pCAT/−449 (containing nucleotides −449 to +199 of the *WT1* promoter) were kind gifts from Dr. Grady Saunders (University of Texas, M.D. Anderson Cancer Center, Houston, TX, USA). The constructs pCAT/−996, pCAT/−910 and pCAT/−733 were generated by PCR amplification using a sense strand oligonucleotide containing a *Hin*dIII site overhang and an antisense

oligonucleotide 3′ to a unique *Hin*dIII site at position −449. The following are the sense strand oligonucleotides used for the indicated constructs: pCAT/−996, hWT1-1S (5′-ataagcttctgagcaaccagaat-3′); pCAT/−910, hWT1-2S (5′-ataagctttcgtatccaaaccc-3′); and pCAT/−733, hWT1-3S (5′-ataagcttaagtgctgctgact-3′). The antisense oligonucleotide used was: hWT1-4AS (5′-agcgcagaaagaactcagtc-3′). The PCR products were digested with *Hin*dIII and cloned into pCAT/−449, which had also been linearized with *Hin*dIII. pCAT/−1101/997, pCAT/−996/911, pCAT/−910/734 and pCAT/−996/734 were constructed by PCR amplification using sense and antisense oligonucleotides with *Hin*dIII overhangs. The following are the sense and antisense oligonucleotides used for the indicated constructs: pCAT/−1101/997, hWT1-5S (5′-ataagcttgagctcccaaagat-3′) and hWT1-6AS (5′-ataagctttgattgaccaggag-3′); pCAT/−996/911, hWT1-1S and hWT1-7AS (5′-ataagcttgcccggcaggga-3′); pCAT/−910/734, hWT1-2S and hWT1-8AS (5′-atatataagcttgtttccctttccag-3′); and pCAT/−996/734, hWT1-1S and hWT1-8AS. Subsequent cloning was carried out as described for pCAT/−996. Plasmid pCAT/Δ(P3-2) was made by performing two separate PCRs, one with hWT1-1S and mutPea3-2/AS (5′-tggcgcccagtttgggg-3′) and the other with mutPea3-2/S (5′-ccaaactgggcgccatgctccggccggaatat-3′) and hWT1-8AS. The products of these PCRs were annealed, extended, and amplified with hWT1-1S and hWT1-8AS, digested with *Hin*dIII, and cloned into pCAT/−449 (which had also been linearized with *Hin*dIII). Plasmid pCAT/Δ(P3-2)(P3-Py) was made by performing two separate PCRs, one with hWT1-1S and mutPea3-3/AS (5′-agtttggggaggagggg-3′) and the other with mutPea3-3/S (5′-ctcctccccaaactcaggctttgggcgtttg-3′) and hWT1-8AS. The products of these PCRs were annealed, extended, and amplified with hWT1-1S and hWT1-8AS. The product was digested with *Hin*dIII and cloned into pCAT/−449, which had been linearized with *Hin*dIII. Plasmid pCAT/Δ(P3-Py) was made by performing two separate PCRs, one with hWT1-1S and mutPea3-4/AS (5′-ggccggagcatcctggc-3′) and the other with mutPea3-4/S (5′-aggatgctccggccatatactcaggctttgg-3′) and hWT1-8AS. The products of these PCRs were then annealed, extended, and amplified with hWT1-1S and hWT1-8AS, digested with *Hin*dIII, and cloned into pCAT/−449 (which had been linearized with *Hin*dIII). All clones were sequenced to verify the integrity of the amplification products.

2.6. Western blots and electrophoretic mobility shift assays (EMSA)

CHO and COS7 cells were transfected with 5 μg of reporter plasmid and the indicated amounts of pRcRSV/*Pea3* expression vector. Cells were harvested as indicated for the CAT assays and 60 μg of total cellular protein was electrophoresed on an 8% sodium dodecyl sulfate–polyacrylamide gel electrophoresis (SDS–PAGE) gel. The gel was electroblotted onto polyvinylidene difluoride (PVDF) membrane and probed with an anti-Pea3 antibody (Santa Cruz Biotechnology), followed by incubation with anti-mouse IgG-horseradish peroxidase-conjugated antibody, as recommended by the manufacturer (Santa Cruz Biotechnology). To visualize protein, blots were incubated in Western Lightning™ Chemiluminescence Reagent Plus according to the manufacturer's instructions (Perkin Elmer Life Sciences) and exposed to Kodak X-OMAT film.

The recombinant fusion protein glutathione *S*-transferase (GST)-Pea3 was expressed in BL21 bacterial cells by isopropyl-β-D-thiogalactose induction from a GST-based expression vector. The protein was purified by affinity chromatography using glutathione-Sepharose 4B beads followed by elution with reduced glutathione, as recommended by the manufacturer (Amersham Pharmacia Biotech). Approximately 1.5 μg of GST-Pea3 was incubated for 20 min at room temperature with 0.04 pmol (30 000–50 000 cpm) of double-stranded oligonucleotide probes labeled by the Klenow reaction using [α-^{32}P]-dCTP. Binding reactions contained 10 mM Tris–HCl (pH 7.5), 2 mM $MgCl_2$, 50 mM NaCl, 1 mM EDTA, 1 mM dithiothreitol, 5% glycerol, 1 μg poly[(dIdC)(dIdC)] and 1 μg salmon sperm DNA. In binding reactions containing unlabeled, competitor DNA, the protein was pre-incubated with the indicated molar excess of specific competitor DNA for 15 min at room temperature prior to the addition of probe. In supershift reactions, the protein was pre-incubated with the indicated antibody for 15 min at room temperature prior to the addition of probe. EMSA binding reactions were electrophoresed into 4% polyacrylamide/0.5×TBE gels in 0.5×TBE buffer (1×TBE is 0.18 M Tris, 0.18 M boric acid, 4 mM EDTA) at 96 V at room temperature. Gels were dried and exposed to Kodak X-OMAT film.

3. Results

3.1. Microarray analysis

In order to identify downstream targets of Pea3, a dominant-negative form, ΔNPea3En, was expressed in MDA-MB-468 cells and was expected to reduce expression of genes constitutively activated by endogenous Pea3. MDA-MB-468 cells were selected for analysis based on their high levels of endogenous Pea3 expression [30]. Of the 22 283 probe sets spotted on the HG-U133A array, 186 probe sets produced normalized signal intensities demonstrating lower expression (greater than

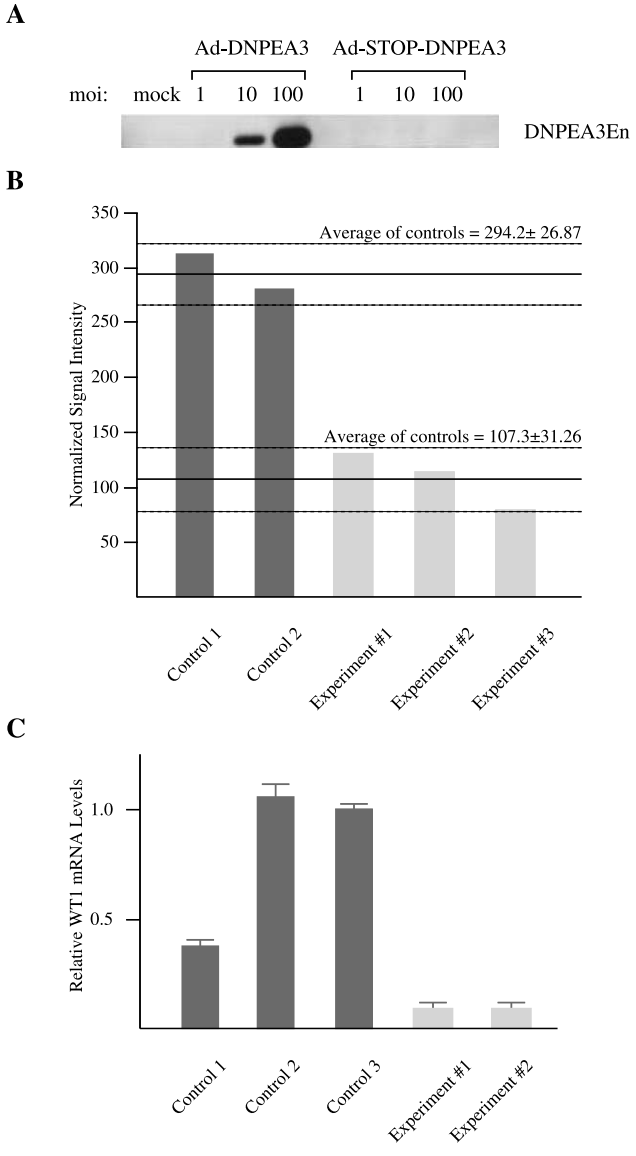

Fig. 1. A: Western blot analysis of DNPea3En expressed in MDA-MB-468 infected cells. B: Normalized signal intensities of probe set corresponding to WT1 mRNA from MDA-MB-468 cells (control) and ΔNPea3En-infected MDA-MB-468 cells (experimental) from microarray experiments. Control and experimental average signal intensities are indicated (solid lines) along with standard deviations (dotted lines). C: Relative levels of WT1 expression in control MDA-MB-468 cells (control) or ΔNPea3En-infected MDA-MB-468 cells (experimental) determined by quantitative PCR. Three independent experimental determinations were made and are expressed relative to the levels obtained with control sample #3. The average error of the mean is also indicated.

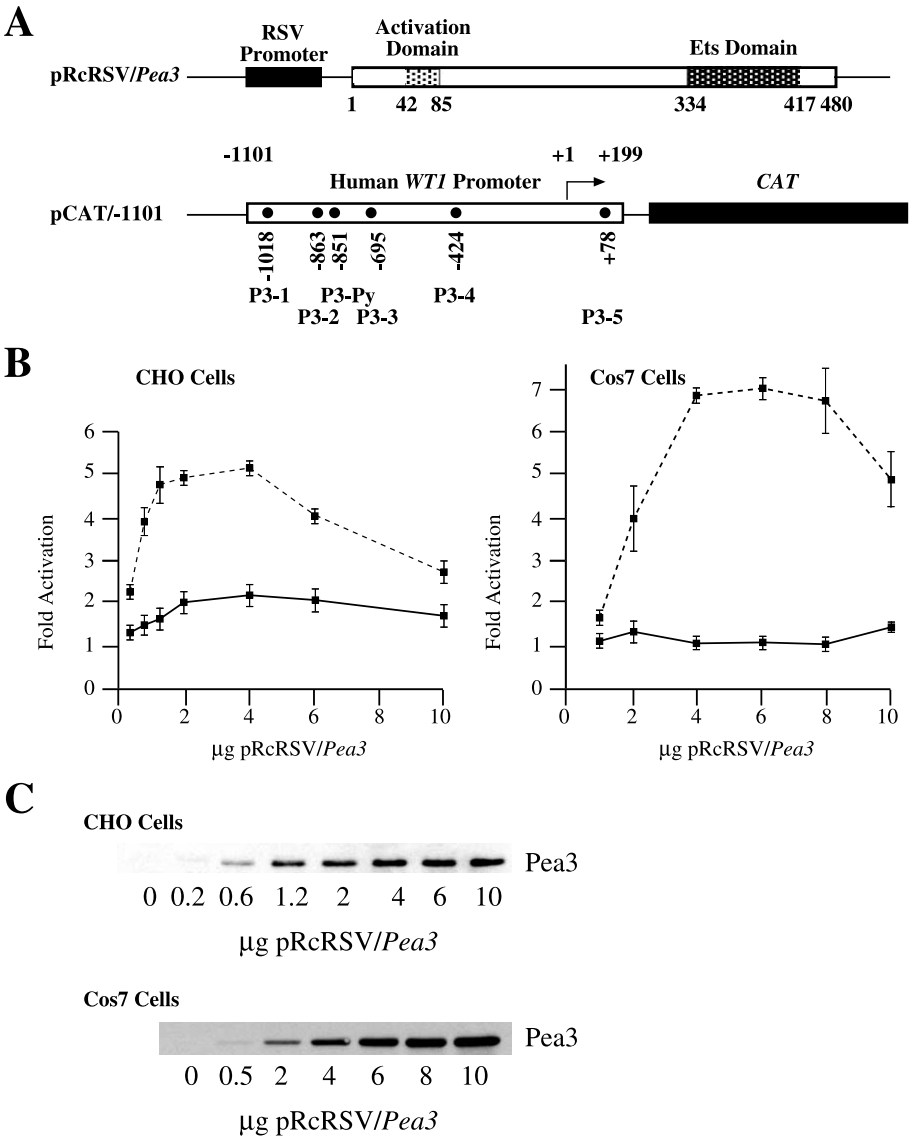

Fig. 2. A: Schematic representation of the expression vector and reporter plasmids used in this study. The pRcRSV/*Pea3* expression vector contains the murine *Pea3* cDNA under control of the RSV promoter to produce a protein of 480 amino acids (66 kDa). The amino-terminal region of Pea3 contains a 43 amino acid acidic activation domain and the carboxy-terminal region contains the ETS DNA binding domain. The reporter plasmid, pCAT/−1101, contains the human *WT1* promoter cloned upstream of the *CAT* gene in the vector pCAT/Basic. The major start site of transcription [31] is indicated by an arrow. The putative Pea3 binding sites within the *WT1* promoter identified by TESS, and their positions relative to the start site of transcription, are indicated and labeled P3-1 to P3-5 and P3-Py. B: Activation of the *WT1* promoter by *Pea3*. Co-transfections in CHO and COS7 cells were performed with 5 µg of reporter plasmid and increasing amounts of pRcRSV/*Pea3* expression vector. The fold transactivation was calculated by taking the CAT activity obtained in the presence of the indicated amount of pRcRSV/*Pea3* relative to the activity obtained in the absence of pRcRSV/*Pea3*, which was set as 1. Error bars represent the S.E.M. obtained from three experiments (performed in duplicate). C: Western blot analysis of Pea3 in transfected cells. Whole cell protein extracts (from B) were separated by SDS–PAGE, transferred onto a PVDF membrane, and blotted with anti-Pea3 antibody. The amount of Pea3 expression vector titrated into the transfections is indicated below the panel. The cellular origin of the lysates is indicated above the panel.

two-fold) in MDA-MB-468 cells infected with Ad-ΔNPea3En, compared to cells infected with the control virus in all six pairwise comparisons. Of these probe sets, 81 showed statistically significant (95% confidence interval) differential expression between control and experimental samples by *t*-test. Probe set 206067_s_at, corresponding to *WT1* transcript variant D mRNA, fell into the last group of probe sets, displaying a *t*-test *P* value of 0.009 and a fold change of −2.74 (Fig. 1B). This suggested downregulation of *WT1* transcripts upon expression of ΔNPea3En in MDA-MB-468 cells.

To verify these results, we performed kinetic reverse transcription (RT) PCR analysis (real-time) on three control and two experimental samples to assess the relative levels of *WT1*. Following normalization of all five samples to β_2-*microglobulin*, the *WT1* levels were determined relative to one of the control samples (Fig. 1C, control #3). Sample control #3 and #2 showed similar levels of *WT1* expression, whereas control sample #1 showed a three-fold lower *WT1* level (Fig. 1C). Both experimental samples showed an eight-fold decrease in *WT1* levels relative to control samples #2 and #3, and a 2.4-fold decrease relative to control sample #1 (Fig. 1C). These experiments validate the array-based expression differences observed for *WT1* and suggest that WT1 may reside downstream of Pea3.

3.2. Identification of Pea3 sites within the WT1 promoter

To characterize the potential regulation of *WT1* by Pea3, we analyzed the *WT1* promoter for candidate Pea3 binding sites. The human *WT1* promoter lacks a TATA box or CCAAT motif and has a GC content of 71% [31]. Four transcriptional start sites clustering within a 32 bp region have been previously identified by mung bean nuclease mapping [31]. The major transcription start site corresponding to the strongest nuclease-resistant band was designated +1. The *WT1* upstream region of −1101 to +199 was submitted to the TESS-String-Based Search that used the TRANSFAC v3.2 database (www.cbil.upenn.edu/tess) for analysis of potential transcription factor binding sites. Five putative Pea3 binding sites were identified at positions −1018, −863, −695, −424 and +78 and were named P3-1 to P3-5 (Fig. 2A). Additionally, a sixth potential Pea3 binding site was identified at −851 (P3-Py) upon visual inspection of the *WT1* promoter (Fig. 2A).

3.3. Transactivation of the WT1 promoter by transient expression of Pea3

To assess whether any of the identified Pea3 binding sites in the *WT1* upstream region were functional, a *WT1/CAT* reporter vector (pCAT/−1101) containing sequences from nucleotides −1101 to +199 was co-transfected with increasing amounts of RSV/*Pea3* expression vector into CHO or COS7 cells to gauge the activation potential of Pea3 (Fig. 2B). Titration of pRcRSV/*Pea3* into CHO cells produced a five-fold transactivation of the pCAT/−1101 promoter at ∼4 μg of input pRcRSV/*Pea3* (Fig. 2B), whereas transactivation of the control pCAT/Basic vector was affected only slightly (two-fold) by the presence of Pea3 (Fig. 2B). A similar dose response with pRcRSV/*Pea3* was obtained in COS7 cells, with the exception that a higher activation (seven-fold) was obtained with 4–8 μg of pRcRSV/*Pea3* (Fig. 2B). No effect of pRcRSV/*Pea3* on the promoterless pCAT/Basic vector was noted in COS7 cells (Fig. 2B). Western blotting analysis performed on total cellular protein extracts from transfected CHO and COS7 cells revealed a quantitative increase in Pea3 protein expression upon titration of pRcRSV/*Pea3*, as expected (Fig. 2C).

3.4. Identification of a Pea3 responsive element within the WT1 promoter

To determine which of the six putative Pea3 binding sites within the −1101 to +199 *WT1* promoter region were mediating Pea3 transactivation, a series of promoter deletion constructs were cloned into the *CAT* reporter plasmid. CHO and COS7 cells were transfected with these in conjunction with a fixed amount of pRcRSV/*Pea3* expression vector (Fig. 3A). The deletion mutant pCAT/−996 was responsive to Pea3 in CHO and COS7 cells, whereas pCAT/−733, pCAT/−449, and pCAT/−996/911 were not responsive to Pea3 in CHO cells (background activation in CHO cells is ∼two-fold [Fig. 2B]) whereas their responsiveness decreased (2.3–3.3-fold), but was not abolished, in COS7 cells (Fig. 3A). The results from these deletion mutants suggested that (a) Pea3 site(s) should reside between nucleotides −910 and −734. This was directly tested with constructs pCAT/−910/734 and pCAT/−996/734, in which this region (nucleotides −910 to −734 or nucleotides −996 to −734) was grafted onto pCAT/−449. Both constructs showed responsiveness to Pea3 in CHO and COS7 cells to levels that resembled those obtained with pCAT/−996 (Fig. 3A).

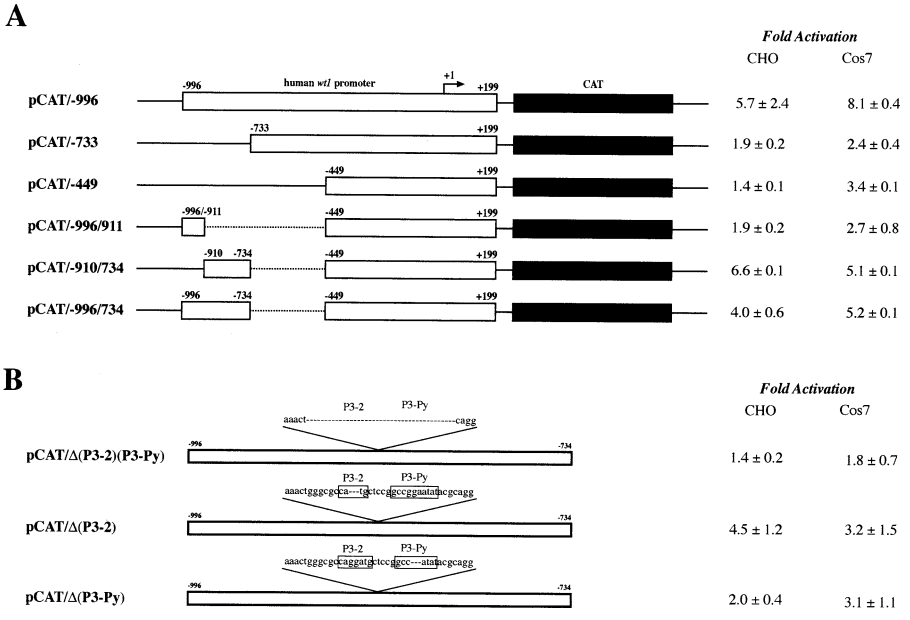

Fig. 3. Analysis of *WT1* promoter deletion mutants for Pea3 transactivation. A: Schematic diagram showing *WT1* promoter deletion constructs. The empty boxes represent the *WT1* promoter and the blackened boxes represent the *CAT* gene. The nucleotide positions of the *WT1* promoter sequences contained in each deletion construct are indicated above the boxes. B: The sequence of deletion mutants within two potential Pea3 sites at nucleotides −996 to −734 are shown above the constructs pCAT/Δ(P3-2), pCAT/Δ(P3-2)(P3-Py) and pCAT/Δ(P3-Py). A dotted line refers to an internal deletion. Adjacent to each reporter construct is the fold transactivation and the S.E.M. (obtained from at least three experiments, each done in duplicate). The fold transactivation was calculated by taking the CAT activity obtained with the reporter construct in the presence of the expression plasmid (pRcRSV/*Pea3*), and dividing by the activity obtained with the reporter in the presence of the empty expression vector.

The sequence between nucleotides −910 and −734 contains two potential Pea3 binding sites – P3-2 and P3-Py (Fig. 2A). To assess the contribution of these sites to the Pea3 transactivation response, reporter plasmids containing mutations at one or both sites were constructed into the pCAT/−996/734 reporter backbone. Deletion of both Pea3 sites generated a reporter, pCAT/Δ(P3-2)(P3-Py), that was no longer responsive to Pea3 in CHO and COS7 cells (Fig. 3B). The reporter pCAT/Δ(P3-Py) was not responsive to Pea3 in CHO cells since the level of activation obtained (two-fold) is similar to levels obtained with the promoterless pCAT/Basic reporter (Fig. 2B). However, in COS7 cells this promoter was still responsive to Pea3. Deletion of the P3-2 site generated a reporter, pCAT/Δ(P3-2), that was responsive to Pea3 in both CHO and COS7 cells (Fig. 3B). The response in COS7 cells was 61% of control levels (i.e. pCAT/−996/734). We interpret these results to indicate that the P3-Py site is required for full responsiveness to Pea3 in CHO cells, whereas in COS7 cells, both P3-2 and P3-Py appear to be required for the full response.

3.5. *Binding of Pea3 to the nucleotide sequences defining the P3-Py site*

To assess whether Pea3 could interact directly with sequences within the *WT1* promoter, we performed a series of mobility shift assays with an oligonucleotide containing both the P3-2 and P3-Py sites (called Pea3-2 in Fig. 4A) and recombinant GST-Pea3 protein. Recombinant Pea3 (as opposed to cell extracts) was utilized in the EMSA to ensure that only *WT1* promoter/Pea3 interactions would be directly analyzed, and not interactions of other ETS protein members with the *WT1* promoter. As positive and negative controls of specific DNA binding, we used oligonucleotides containing an optimal Pea3 binding site (called Pea3 in Fig. 4A) and an oligonucleotide with a mutated Pea3 binding site (called Mut1 in Fig. 4A). Incubation of GST-Pea3 with radiolabeled Pea3-2 produced a single complex (indicated by an arrow in Fig. 4B; compare lane 1 to 9). This complex can be specifically competed by increasing amounts of unlabeled Pea3-2 oligonucleotide (Fig. 4B, lanes 2–6) and by 100-fold excess of Pea3 oligonucleotide (Fig. 4B, lane 7), but not by 100-fold excess of Mut1 oligonucleotide (Fig. 4B, lane 8). These results indicate that the complex formed by GST-Pea3 on the Pea3-2 oligonucleotide is specific.

To eliminate the possibility that an *Escherichia coli* protein contaminating the GST-Pea3 protein preparation was responsible for the observed complex, we performed the EMSA in the presence of anti-Pea3 antibodies (Fig. 4C). The mobility of the GST-Pea3/Pea3-2 complex is shifted to a slower migrating species in the presence of anti-Pea3 antibodies (Fig. 4C, compare lane 5 to lane 1). This phenomenon is not observed in the presence of anti-Sp1 antibodies (Fig. 4C, compare lane 6 to lane 1). These results are consistent with GST-Pea3 being present in the complex formed on the Pea3-2 oligonucleotide. GST-ΔC317 is a carboxy-terminal deletion mutant of GST-Pea3 that lacks the ETS domain [25] and therefore cannot form a complex with a Pea3 DNA binding site. Incubation of GST-ΔC317 with radiolabeled Pea3-2 did not produce a complex (Fig. 4C, compare lane 7 to lane 1) indicating that the ETS domain of Pea3 is involved in binding to the Pea3-2 oligonucleotide. Incubation of GST alone with radiolabeled Pea3-2 did not produce a complex (Fig. 4C, compare lane 8 with lane 1), indicating that the GST portion of the GST-Pea3 fusion protein is not responsible for the observed complex between GST-Pea3 and Pea3-2.

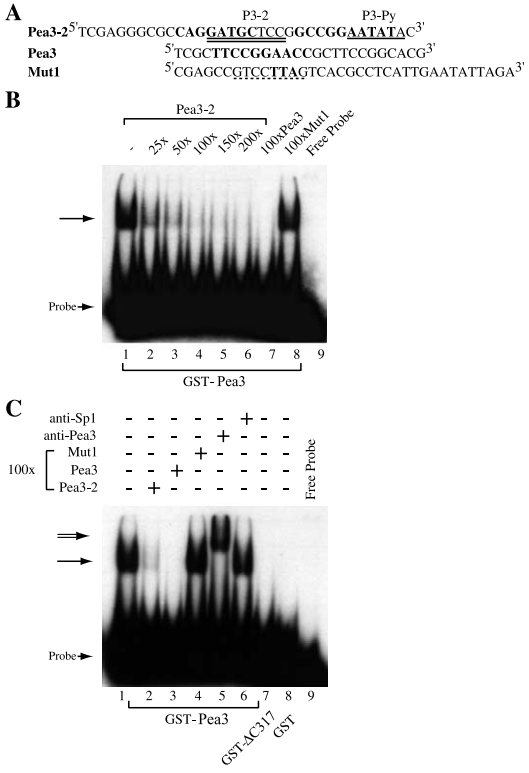

Fig. 4. EMSA demonstrating specific binding of Pea3 to the *WT1* promoter sequences. A: Sequences of the oligonucleotides used to analyze DNA binding of Pea3. Pea3-2 is an oligonucleotide containing the putative P3-2 binding site (double underline) identified by TESS within the −996 to −734 region of the *WT1* promoter, and the P3-Py site (single underline). The Pea3 oligonucleotide contains a known Pea3 binding site and was used as a positive control (J. Hassell, personal communication). The core Pea3 site is shown in bold. Mut1 is an oligonucleotide containing a mutant Pea3 binding site used as a negative control (sequence underlined, mutation in bold). B: Pea3 can interact with sequences within the *WT1* promoter. Binding of GST-Pea3 to radiolabeled Pea3-2 (lane 1) and competition of this complex by increasing amounts of unlabeled Pea3-2 oligonucleotide (lanes 2–6). Binding reactions with radiolabeled Pea3-2 and competition with oligonucleotide Pea3 (lane 7) and oligonucleotide Mut1 (lane 8) are also shown. The nature of the specific competitor oligonucleotide, and the molar amount used relative to the radiolabeled Pea3-2 probe, is indicated above each reaction lane. The position of migration of the specific complex is indicated by an arrow and that of the probe shown by an arrowhead. C: Supershift of the Pea3 complex with an anti-Pea3 antibody. The nature of the specific competitor oligonucleotide, of the antibody, and of the GST protein used in the EMSA is indicated. The specific GST-Pea3/DNA complex is indicated by an arrow, the supershifted complex by a double arrow, and the free probe by an arrowhead.

To further delineate which of the Pea3 binding sites within Pea3-2 (and hence between nucleotides −910 and −734 of the *WT1* promoter) could interact with Pea3, EMSAs were performed using a series of mutant oligonucleotides as probes and recombinant GST-Pea3 (Fig. 5). EMSAs performed with Mut5 (which lacks the P3-2 site) generated a complex that could not be competed with Mut7 (which lacks both P3-2 and P3-Py sites) but which could be supershifted with anti-Pea3 antibodies (Fig. 5B, lanes 1–3). The complex formed on Mut5 behaved similarly to the complex formed on Pea3-2

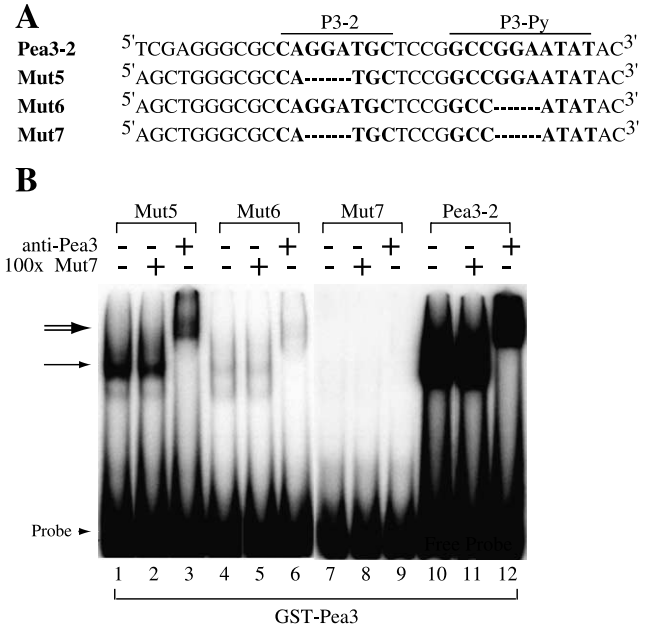

Fig. 5. Analysis of Pea3 binding sites on oligonucleotide Pea3-2. A: Sequences of the oligonucleotides used to analyze DNA binding of Pea3. Mut5 is a mutant of the Pea3-2 oligonucleotide containing a mutation within the P3-2 binding site. Mut6 is a mutant of the Pea3-2 oligo containing a mutation in the P3-Py binding site. Mut7 is a mutant version of Pea3-2 containing deletions in both the P3-2 and P3-Py sites. B: EMSA using Mut5, Mut6, and Mut7 as probes to analyze binding by GST-Pea3. EMSAs were performed in the presence of GST-Pea3 and the indicated oligonucleotides. The nature of the competitor oligonucleotide or antibody used in the EMSA is indicated above each lane. The specific GST-Pea3/DNA complex is indicated by an arrow, the supershifted complex by a double arrow, and the free probe by an arrowhead.

(Fig. 5B, compare lanes 1–3 to lanes 10–12). A faint, diffuse complex was formed on Mut6 (which lacks the P3-Py site) (lane 4) and appeared to be specific, as it was not competed by Mut7 (lane 5) and was supershifted by anti-Pea3 antibodies (lane 6). Mut7 was unable to form a complex with GST-Pea3 (lanes 7–9). Hence, these data suggest that Pea3 binds preferentially to the P3-2 site.

4. Discussion

The analysis described in this report indicates that the *WT1* promoter can be transactivated by Pea3 and that this effect is mediated through a region containing two Pea3 sites. We found that the *WT1* promoter was responsive to Pea3 in both CHO and COS7 cells (Fig. 2). To identify the *cis*-acting element(s) within the *WT1* promoter responsible for mediating the Pea3 response, we generated a series of deletion constructs and assessed their responsiveness to Pea3 (Fig. 3). These experiments indicated that a single site, P3-Py, could mediate the Pea3 effect in CHO cells. However, in COS7 cells, deletion of both P3-2 and P3-Py was necessary to completely abrogate the Pea3 response (Fig. 3). GST-Pea3 can interact directly with the P3-Py element, but weakly with the P3-2 element (Figs. 4 and 5) suggesting that in COS7 cells, the P3-2 site may be used by other ETS family members. Our experiments also do not exclude the possibility of there being additional functional Pea3 responsive sites within the *WT1* promoter, as is possibly suggested by the 'residual' activation levels observed in COS7 with pCAT/−449 (Fig. 3A).

Our studies define an additional layer of complexity to the transcriptional network regulating *WT1* expression. Enhancer and silencer elements have been mapped: (i) 15 kb [32] and 1.3 kb [33] upstream of the *WT1* transcription initiation sites, (ii) within the third intron [33,34], and (iii) downstream of the *WT1* gene [35]. *WT1* expression is known to be regulated by at least six different transcription factors: Sp1, GATA-1, NF-κB, WT1, Pax2, and Pax8. Both the human and murine *WT1* promoters lack a TATA box and CCAAT site and are GC-rich [15,31]. DNase I footprinting analysis revealed the presence of multiple sites within the *WT1* regulatory region (promoter and 5′ untranslated region [UTR]) protected by Sp1, and co-transfection experiments confirmed the ability of Sp1 to activate through these sites [20,31]. *WT1* expression in the lymphoid system is influenced by GATA-1 activation through hematopoietic-specific enhancers found within the third intron and within the 3′ UTR of the *WT1* gene [34,35]. NF-κB activates *WT1* expression through a site downstream of the *WT1* major transcription start site [36], possibly also contributing to *WT1* gene expression during hematopoiesis.

WT1 is thought to repress its own expression by binding to multiple sites within its regulatory region [21]. Two members of the Pax family of transcription factors, Pax2 and Pax8, are also upstream regulators of *WT1* gene expression. Studies with the human and murine promoters have defined Pax8 sites upstream of the major transcription start site through which Pax8 can activate the *WT1* promoter [16,19]. Pax2 has also been shown to activate *WT1* gene expression. One Pax2 site has been defined on the murine promoter to be present upstream of the major transcription start site, and two other sites have been defined for the human promoter, one positioned upstream and the other downstream of the major transcription start site [17,18]. In turn, WT1 has been shown to be a repressor of the *Pax2* promoter [37]. This reciprocal control of gene expression between WT1 and Pax2 is consistent with the temporal and spatial pattern of *WT1* and *Pax2* gene expression during kidney development [37]. Our results position Pea3 upstream of *WT1* and the next challenge will be to elucidate the interaction network between WT1 *trans*-acting factors.

The physiological relevance of *WT1* induction by Pea3 may be quite significant. The expression patterns of *WT1* and *Pea3* demonstrate a high degree of coincidence during kidney and mammary gland development. Additionally, both WT1 and Pea3 have been implicated in the process of epithelialization through the regulation of downstream target genes required for this process. Specifically, both *WT1* and *Pea3* are expressed in the condensed mesenchymal cells throughout nephrogenesis [14,15,27,38]. In the *WT1* knock-out mouse, there is no outgrowth of the ureteric bud and the mesenchymal cells fail to differentiate and die due to apoptosis [12]. The inability of the mesenchymal cells to differentiate and the failure of the ureteric bud to grow from the Wolffian duct are due to an autonomous cell defect resulting from the loss of *WT1* [12]. WT1 therefore plays an important role in allowing mesenchymal–epithelial interactions to occur during the initial stages of metanephric kidney development. *Pea3* is expressed in several tissues and organs during embryonic development and in the adult mouse [27]. Within a given developing organ, *Pea3*′s expression coincides with regions of the embryo undergoing

cellular proliferation and migration. Like WT1, *Pea3* is expressed in tissues and organs at sites of mesenchymal–epithelial transitions, such as the kidney.

Pea3 and *WT1* are co-expressed in the myoepithelial cells of ducts and alveoli of the mammary gland [10,39]. *Pea3* is also expressed in the terminal end buds of the developing mammary gland [27], whereas WT1 is present in less differentiated cells of the mammary ducts [10]. Since our data suggest that Pea3 resides upstream of *WT1*, activation of *WT1* by Pea3 may be important for mammary gland homeostasis or regulation of ductal and/or alveolar development. Additionally, analysis of *WT1* and *Pea3* expression in mammary tumors has suggested that these two genes may also have a role in mammary oncogenesis. *Pea3* mRNA levels are increased in mammary tumors of transgenic mice expressing either the *neu* oncogene or the polyomavirus *middle T antigen* oncogene under control of the mouse mammary tumor virus promoter [40]. Similarly, *Pea3* mRNA levels are elevated in human breast tumors [41]. Pea3's role in tumorigenesis may be through the regulation of expression of proteases required for the degradation of the extracellular matrix. Deregulated expression of such proteases has been associated with the ability of tumor cells to metastasize [42]. This probably accounts for the metastatic potential of Pea3 overexpressing cells lines that indeed, also overexpress the matrix metalloproteinases (MMPs) MMP-3 and MMP-9 [43]. Ectopic expression of Pea3 in the human breast cancer cell line MCF7 increases the metastatic potential of these cells [44]. Conversely, expression of antisense Pea3 in human tumor cells reduces their invasiveness [45].

On the other hand, studies with WT1 have shown that *WT1* expression levels are either upregulated or downregulated in breast tumors, depending on the tumor type and the stage of the cancer [10,11]. Furthermore, there is altered expression of WT1 in certain human breast tumors [10] with some tumor cells showing cytoplasmic retention, rather than nuclear localization, of WT1. Studies using RT-PCR showed that *WT1* transcript levels are elevated in primary carcinomas and invasive ductal carcinomas compared to normal mammary tissue and have correlated high levels of *WT1* mRNA with poorer prognosis in breast cancer patients [46,47]. WT1 protein levels were found to be correlated with the proliferation of breast cancer cells and downregulation of WT1 protein through the use of antisense oligonucleotides leads to breast cancer growth inhibition and reduced cyclin D1 protein levels [48]. Hence, our data would suggest that overexpression of *Pea3* in some breast cancers may be responsible for elevated *WT1* levels, which in turn could contribute to the increased proliferation of transformed cells.

Unlike the *WT1* homozygous null mouse, the *Pea3* knockout mouse does not have a kidney defect [12,49]. It is possible that the other Pea3 family members, *Erm* and *Er81*, are compensating for the loss of *Pea3* during nephrogenesis. *Erm* is co-expressed with *Pea3* in the condensed metanephric mesenchyme during nephrogenesis and *Er81* is transiently expressed in the metanephric mesenchyme, with its expression peaking at embryonic day 15.5 [27]. Female mice lacking a functional *Pea3* allele of mixed strain background (BALB/c and Sv129) have reduced postnatal branching of the mammary ductal tree prior to puberty and during pregnancy, whereas the mammary glands of pubertal PEA3 null mice of pure strain background (FVB/N) comprise an increased number of terminal end buds and an increased proportion of proliferating cells in their terminal end buds [39]. To our knowledge, mammary duct development has not been closely analyzed in the *WT1* knock-out mouse.

During renal development, a constant remodeling of the extracellular matrix is required to allow invasion and branching of the ureteric bud in the metanephric mesenchyme, suggesting a role for matrix-degrading enzymes, such as matrix MMPs. MMP-1 and MMP-9 are expressed in the metanephric mesenchyme and have been implicated in controlling branching morphogenesis during kidney development [50,51]. E1A-F, the human homolog of mouse Pea3, upregulates the expression of MMP-1, MMP-3 and MMP-9 [52]. Furthermore, Pea3 activates MMP-7 transcription synergistically with β-catenin-Tcf/LEF-1 (T-cell factor/lymphoid enhancer factor-1) [53]. Our data place Pea3 upstream of *WT1*, which in turn could activate the epithelialization program. WT1 is required to regulate the expression of *syndecan-1* and *E-cadherin* [54,55] – proteins that are necessary for triggering signalling events during mesenchymal–epithelial transition. Loss of expression of either gene in epithelial cells causes the cells to lose their epithelial morphology [56–64]. Hence, the coupling of *MMP* activation (by Pea3) and of *syndecan-1* and *E-cadherin* activation (by WT1) ensures co-incident temporal expression of both these processes during renal development. Our results identify Pea3 as a WT1 *trans*-acting factor, important for mesenchymal–epithelial transitions.

Acknowledgements: M.T.D. was supported by scholarships from FRSQ-FCAR (Fonds de la recherche en santé du Quebec-Fonds pour la formation de chercheurs et l'aide à la recherche) and the McGill University Faculty of Medicine during the course of this work. J.P. is a Canadian Institutes of Health Research (CIHR) Senior Investigator. This work was supported by grants from the Canadian Institutes of Health Research (CIHR) to J.P. and J.A.H. and grants to J.A.H. from the Canadian Breast Cancer Research Alliance and the DOD Breast Cancer Research Program, DAMD17-02-1-0480.

References

[1] Matsunaga, E. (1981) Hum. Genet. 57, 231–246.
[2] Varanasi, R., Bardeesy, N., Ghahremani, M., Petruzzi, M.J., Nowak, N., Adam, M.A., Grundy, P., Shows, T.B. and Pelletier, J. (1994) Proc. Natl. Acad. Sci. USA 91, 3554–3558.
[3] Pelletier, J., Bruening, W., Kashtan, C.E., Mauer, S.M., Manivel, J.C., Striegel, J.E., Houghton, D.C., Junien, C., Habib, R., Fouser, L., Fine, R.N., Silverman, B.L., Haber, D.A. and Housman, D. (1991) Cell 67, 437–447.
[4] Lee, S.B. and Haber, D.A. (2001) Exp. Cell Res. 264, 74–99.
[5] Rauscher III, F.J., Morris, J.F., Tournay, O.E., Cook, D.M. and Curran, T. (1990) Science 250, 1259–1262.
[6] Wang, Z.Y., Qiu, Q.Q., Enger, K.T. and Deuel, T.F. (1993) Proc. Natl. Acad. Sci. USA 90, 8896–8900.
[7] Fraizer, G.C., Patmasiriwat, P., Zhang, X. and Saunders, G.F. (1995) Blood 86, 4704–4706.
[8] Moore, A.W., McInnes, L., Kreidberg, J., Hastie, N.D. and Schedl, A. (1999) Development 126, 1845–1857.
[9] Wagner, K.D., Wagner, N., Vidal, V.P., Schley, G., Wilhelm, D., Schedl, A., Englert, C. and Scholz, H. (2002) EMBO J. 21, 1398–1405.
[10] Silberstein, G.B., Van Horn, K., Strickland, P., Roberts, C.T.Jr. and Daniel, C.W. (1997) Proc. Natl. Acad. Sci. USA 94, 8132–8137.
[11] Silberstein, G.B., Dressler, G.R. and Van Horn, K. (2002) Oncogene 21, 1009–1016.
[12] Kreidberg, J.A., Sariola, H., Loring, J.M., Maeda, M., Pelletier, J., Housman, D. and Jaenisch, R. (1993) Cell 74, 679–691.
[13] Herzer, U., Crocoll, A., Barton, D., Howells, N. and Englert, C. (1999) Curr. Biol. 9, 837–840.

[14] Pritchard-Jones, K., Fleming, S., Davidson, D., Bickmore, W., Porteous, D., Gosden, C., Bard, J., Buckler, A., Pelletier, J., Housman, D., van Heyningen, V. and Hastie, N. (1990) Nature 346, 194–197.
[15] Pelletier, J., Schalling, M., Buckler, A.J., Rogers, A., Haber, D.A. and Housman, D. (1991) Genes Dev. 5, 1345–1356.
[16] Dehbi, M. and Pelletier, J. (1996) EMBO J. 15, 4297–4306.
[17] Dehbi, M., Ghahremani, M., Lechner, M., Dressler, G. and Pelletier, J. (1996) Oncogene 13, 447–453.
[18] McConnell, M.J., Cunliffe, H.E., Chua, L.J., Ward, T.A. and Eccles, M.R. (1997) Oncogene 14, 2689–2700.
[19] Fraizer, G.C., Shimamura, R., Zhang, X. and Saunders, G.F. (1997) J. Biol. Chem. 272, 30678–30687.
[20] Cohen, H.T., Bossone, S.A., Zhu, G., McDonald, G.A. and Sukhatme, V.P. (1997) J. Biol. Chem. 272, 2901–2913.
[21] Rupprecht, H.D., Drummond, I.A., Madden, S.L., Rauscher III, F.J. and Sukhatme, V.P. (1994) J. Biol. Chem. 269, 6198–6206.
[22] Xin, J.H., Cowie, A., Lachance, P. and Hassell, J.A. (1992) Genes Dev. 6, 481–496.
[23] de Launoit, Y., Baert, J.L., Chotteau, A., Monte, D., Defossez, P.A., Coutte, L., Pelczar, H. and Leenders, F. (1997) Biochem. Mol. Med. 61, 127–135.
[24] Graves, B.J. and Petersen, J.M. (1998) Adv. Cancer Res. 75, 1–55.
[25] Bojovic, B.B. and Hassell, J.A. (2001) J. Biol. Chem. 276, 4509–4521.
[26] Greenall, A., Willingham, N., Cheung, E., Boam, D.S. and Sharrocks, A.D. (2001) J. Biol. Chem. 276, 16207–16215.
[27] Chotteau-Lelievre, A., Desbiens, X., Pelczar, H., Defossez, P.A. and de Launoit, Y. (1997) Oncogene 15, 937–952.
[28] Shepherd, T.G., Kockeritz, L., Szrajber, M.R., Muller, W.J. and Hassell, J.A. (2001) Curr. Biol. 11, 1739–1748.
[29] Anton, M. and Graham, F.L. (1995) J. Virol. 69, 4600–4606.
[30] Baert, J.L., Monte, D., Musgrove, E.A., Albagli, O., Sutherland, R.L. and de Launoit, Y. (1997) Int. J. Cancer 70, 590–597.
[31] Hofmann, W., Royer, H.D., Drechsler, M., Schneider, S. and Royer-Pokora, B. (1993) Oncogene 8, 3123–3132.
[32] Scholz, H., Bossone, S.A., Cohen, H.T., Akella, U., Strauss, W.M. and Sukhatme, V.P. (1997) J. Biol. Chem. 272, 32836–32846.
[33] Hewitt, S.M., Fraizer, G.C. and Saunders, G.F. (1995) J. Biol. Chem. 270, 17908–17912.
[34] Zhang, X., Xing, G., Fraizer, G.C. and Saunders, G.F. (1997) J. Biol. Chem. 272, 29272–29280.
[35] Fraizer, G.C., Wu, Y.J., Hewitt, S.M., Maity, T., Ton, C.C., Huff, V. and Saunders, G.F. (1994) J. Biol. Chem. 269, 8892–8900.
[36] Dehbi, M., Hiscott, J. and Pelletier, J. (1998) Oncogene 16, 2033–2039.
[37] Ryan, G., Steele-Perkins, V., Morris, J.F., Rauscher III, F.J. and Dressler, G.R. (1995) Development 121, 867–875.
[38] Armstrong, J.F., Pritchard-Jones, K., Bickmore, W.A., Hastie, N.D. and Bard, J.B. (1993) Mech. Dev. 40, 85–97.
[39] Kurpios, N.A., Sabolic, N.A., Shepherd, T.G., Fidalgo, G.M. and Hassell, J.A. (2003) J. Mamm. Gland Biol. Neopl. 8, 175–189.
[40] Trimble, M.S., Xin, J.H., Guy, C.T., Muller, W.J. and Hassell, J.A. (1993) Oncogene 8, 3037–3042.
[41] Benz, C.C., O'Hagan, R.C., Richter, B., Scott, G.K., Chang, C.H., Xiong, X., Chew, K., Ljung, B.M., Edgerton, S., Thor, A. and Hassell, J.A. (1997) Oncogene 15, 1513–1525.
[42] Chambers, A.F. and Matrisian, L.M. (1997) J. Natl. Cancer Inst. 89, 1260–1270.
[43] Shindoh, M., Higashino, F., Kaya, M., Yasuda, M., Funaoka, K., Hanzawa, M., Hida, K., Kohgo, T., Amemiya, A., Yoshida, K. and Fujinaga, K. (1996) Am. J. Pathol. 148, 693–700.
[44] Kaya, M., Yoshida, K., Higashino, F., Mitaka, T., Ishii, S. and Fujinaga, K. (1996) Oncogene 12, 221–227.
[45] Hida, K., Shindoh, M., Yasuda, M., Hanzawa, M., Funaok, K., Kohgo, T., Amemiya, A., Totsuka, Y., Yoshida, K. and Fujinaga, K. (1997) Am. J. Pathol. 150, 2125–2132.
[46] Loeb, D.M., Evron, E., Patel, C.B., Sharma, P.M., Niranjan, B., Buluwela, L., Weitzman, S.A., Korz, D. and Sukumar, S. (2001) Cancer Res. 61, 921–925.
[47] Miyoshi, Y., Ando, A., Egawa, C., Taguchi, T., Tamaki, Y., Tamaki, H., Sugiyama, H. and Noguchi, S. (2002) Clin. Cancer Res. 8, 1167–1171.
[48] Zapata-Benavides, P., Tuna, M., Lopez-Berestein, G. and Tari, A.M. (2002) Biochem. Biophys. Res. Commun. 295, 784–790.
[49] Laing, M.A., Coonrod, S., Hinton, B.T., Downie, J.W., Tozer, R., Rudnicki, M.A. and Hassell, J.A. (2000) Mol. Cell. Biol. 20, 9337–9345.
[50] Lelongt, B., Trugnan, G., Murphy, G. and Ronco, P.M. (1997) J. Cell Biol. 136, 1363–1373.
[51] Sakurai, H. and Nigam, S.K. (1997) Am. J. Physiol. 272, F139–146.
[52] Higashino, F., Yoshida, K., Noumi, T., Seiki, M. and Fujinaga, K. (1995) Oncogene 10, 1461–1463.
[53] Crawford, H.C., Fingleton, B., Gustavson, M.D., Kurpios, N., Wagenaar, R.A., Hassell, J.A. and Matrisian, L.M. (2001) Mol. Cell. Biol. 21, 1370–1383.
[54] Cook, D.M., Hinkes, M.T., Bernfield, M. and Rauscher III, F.J. (1996) Oncogene 13, 1789–1799.
[55] Hosono, S., Gross, I., English, M.A., Hajra, K.M., Fearon, E.R. and Licht, J.D. (2000) J. Biol. Chem. 275, 10943–10953.
[56] Vainio, S., Lehtonen, E., Jalkanen, M., Bernfield, M. and Saxen, L. (1989) Dev. Biol. 134, 382–391.
[57] Vainio, S., Jalkanen, M., Bernfield, M. and Saxen, L. (1992) Dev. Biol. 152, 221–232.
[58] Ekblom, P. (1981) J. Cell Biol. 91, 1–10.
[59] Vestweber, D., Kemler, R. and Ekblom, P. (1985) Dev. Biol. 112, 213–221.
[60] Kato, M., Saunders, S., Nguyen, H. and Bernfield, M. (1995) Mol. Biol. Cell 6, 559–576.
[61] Leppa, S., Mali, M., Miettinen, H.M. and Jalkanen, M. (1992) Proc. Natl. Acad. Sci. USA 89, 932–936.
[62] Behrens, J., Mareel, M.M., Van Roy, F.M. and Birchmeier, W. (1989) J. Cell Biol. 108, 2435–2447.
[63] Birchmeier, W., Behrens, J., Weidner, K.M., Frixen, U.H. and Schipper, J. (1991) Curr. Opin. Cell Biol. 3, 832–840.
[64] Berx, G., Becker, K.F., Hofler, H. and van Roy, F. (1998) Hum. Mutat. 12, 226–237.